MECSOL 2022 - Proceedings of the 8th International Symposium on Solid Mechanics
M.L. Bittencourt, J. Labaki, L.C.M. Vieira Jr. and E. Mesquita (Editors), Campinas SP, Brazil, October 17th to 19th, 2022

Influence of Sloshing on the Dynamic Behavior of a Launcher Vehicle Submitted to Transient Loads

Domingos Sávio Aguiar [1], Carlos d'Andrade Souto [1], Maurício Guimaraes da Silva[1]

[1] Institute of Aeronautics and Space – IAE, São José dos Campos – São Paulo, Brasil -12228-904.
domingosdsa@fab.mil.br, soutocds@fab.mil.br, mauriciomgs@fab.mil.br.

Abstract: Liquid-propellant rocket motors are widely used in satellite launch rockets because of their high specific impulse (compared to solid-propellant motors) and the ability to control the magnitude of thrust, including in-flight shutdown and restart. During its whole mission a launch vehicle is submitted to different dynamic loads and the resultant response may be affected by the liquid mass in the propellant tanks. In this sense, the lateral transient loads such as wind gusts and control forces cause oscillations of the launch vehicle and the dynamic behavior analysis with sloshing effects is of great importance during different phases of the project. A liquid mass with a free surface in a reservoir subjected to displacements may suffer the phenomenon of "sloshing", which consists of oscillations of the liquid free surface. Also, when certain kinds of sloshing modes are excited, the liquid volume center of mass position can be shifted. Since the liquid propellants mass in a launcher can be significant in relation to the whole vehicle mass, oscillations in the fluid volumes can lead to important dynamic effects. In this work, the dynamic behavior of a launch vehicle is analyzed when the vehicle is submitted to lateral transient loads caused by discrete wind gusts during ascent flight. The influence of liquid propellant on the vehicle dynamics is taken into account considering lateral sloshing effects. The launch vehicle body is modelled as a finite element beam and the liquid slosh mass is modelled as a spring-mass system. It is shown that for different fill ratios of the propellant tanks submitted to the same transient load caused by gust wind, the presence of slosh mass increases the lateral accelerations along the vehicle body.

Keywords: launch vehicle, sloshing, dynamics, transient load, finite element.

INTRODUCTION

A liquid mass with a free surface in a reservoir subjected to displacements may suffer the phenomenon of "sloshing", which consists of oscillations of the liquid free surface.

From an engineering point of view, this phenomenon can be quite significant for storage tanks positioned directly on the ground or at high elevations on supporting structures subjected to seismic loads. In the case of vehicles, the presence of large masses of liquid can affect the dynamic behavior of the system. The greater the fraction of fuel in the total mass, the more relevant sloshing becomes in vehicle dynamics. Thus, due to the large use of liquid-propellant rocket engines, and the large fraction of the propellants in their total mass, as can be seen in Fig. 1, launch vehicles will be particularly susceptible to sloshing.

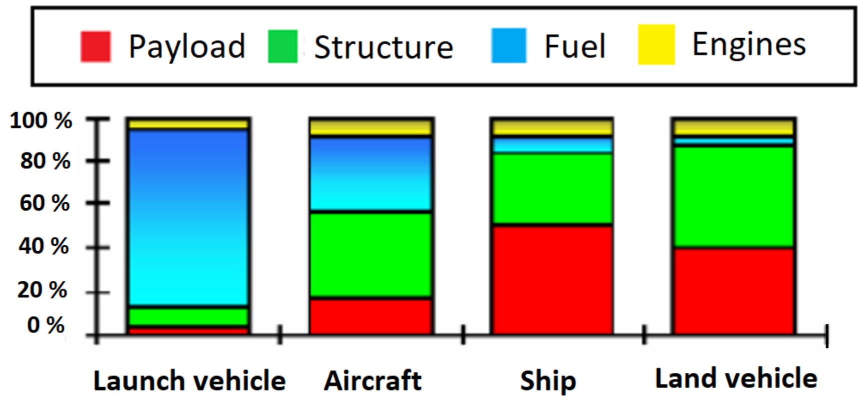

Figure 1 – Mass fraction of fuel in different types of vehicles (Adapted from Shimote, 2005)

A practical way to analyze sloshing effects on a launch vehicle consists of conceptually replace the liquid by an equivalent linear mechanical system, and thus including the dynamic effects of sloshing in the launcher dynamic model, as pointed out in Barrows and Orr (2021).

Considering the methodology described above, recently Aguiar and Souto (2021) presented a study on a launch vehicle with slosh effects. In this work, a conceptual launch vehicle proposed by (Zhuang and Yulin, 2021) is analyzed. A finite element model using beam elements was constructed with the Nx Nastran, (2014) package software. The slosh parameters of propellant tanks were calculated based on linear theory according to Abramson (1966), Ibrahim (2005), and Dodge (2000). The natural frequencies and mode shapes of the vehicle with and without including the liquid slosh mass and sloshing modes and bending modes were calculated for different fill ratios of the propellant tanks.

During its whole mission a launch vehicle is submitted to different dynamic loads, as described in NASA-HDBK, (2001), and its response can be affected by the liquid mass in the propellant tanks. In that sense, the lateral transient loads such as wind gusts and control forces cause oscillations of the launch vehicle and the dynamic behavior analysis with sloshing effects is of great importance during different phases of project. As an example, Steny et al. (2020) discusses dynamic loads estimation for launch vehicles during atmospheric phase, considering transient loads such as a discrete wind gust and control forces, and its dynamics effects are established with respect to rigid body loads. In another study, Jayasidhan et al., (2015) performed transient analysis on launch vehicle where different conditions of discrete wind gust loads were evaluated in order to obtain the more critical condition. An overview of the loads on a launch vehicle can be seen in Fig. 2 extracted from Suresh and Sivan, 2015.

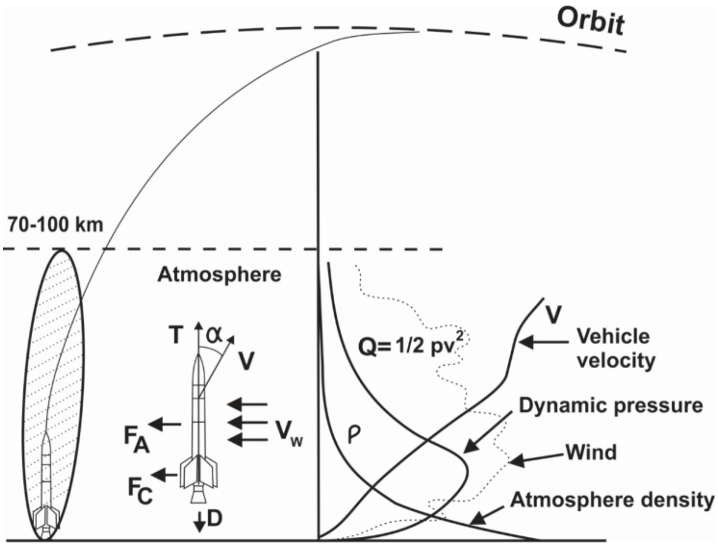

T-Thrust, F_A – Aerodynamic force, F_C – Control force, D – Drag, V - Velocity

Figure 2 – Criticalities of atmospheric flight phase (Extracted from Suresh and Sivan, 2015)

In the last two references previously cited, the slosh was not considered for structural dynamics analysis. Therefore, this work seeks to evaluate this effect when the launch vehicle is submitted to discrete wind gust. The effects of wind gust are transformed into transient aerodynamics forces distributed along vehicle body for the maximum dynamic pressure flight condition. Different fill ratios of the propellant tanks are considered for only the specific aerodynamic transient load since the main aim consist of a sensitive analysis of the slosh mass effects. The transient acceleration responses are calculated in different stations of the vehicle model using direct transient response analysis.

Mechanical slosh model

In the present study, the lateral slosh model for a cylindrical tank partially filled liquid propellant was used, Fig. 3. The geometry of the cylindrical tank consists of its height, *H*, and diameter, *d*. Its volume depends on fill of the tank when the actual liquid level is equal to *h*.

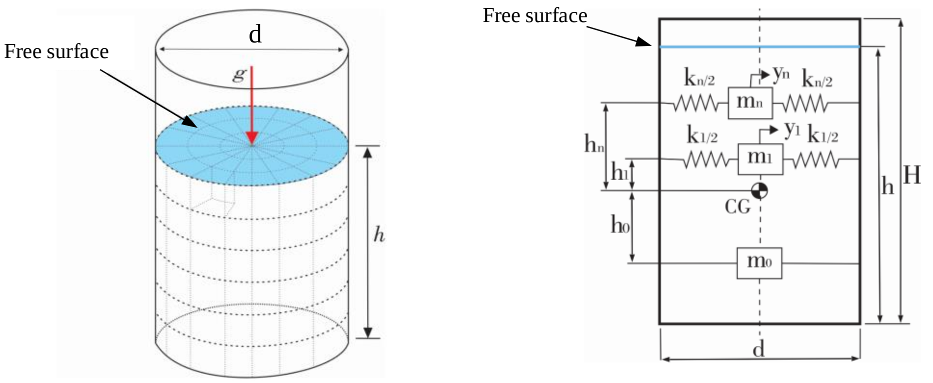

(a) (b)

Figure 3 – Spring-mass slosh model (a) cylindrical tank and (b) mechanical model equivalent

According to linear theory in Abramson (1966) the action of lateral sloshing, represented by a set of spring-mass systems, it causes the displacement, y_n, of slosh mass, m_n, with respect to the tank wall. Each of the spring constant, k_n is chosen such their ratio to the oscillating mass is equal to the square of natural frequency, ω_n^2, of that mode, that is:

$$\omega_n^2 = \frac{k_n}{m_n} = \frac{2\xi_n}{d} tanh\left(\frac{\xi_n h}{d}\right) \tag{1}$$

where the parameters m_n and k_n are given by:

$$m_n = m_{liq}\left[\frac{d}{h\left(\xi_n^2 - 1\right)}\right]\left[tanh\left(\frac{2\xi_n h}{d}\right)\right] \tag{2}$$

$$k_n = m_{liq}\left[\frac{2g}{h\left(\xi_n^2 - 1\right)}\right]\left[tanh\left(\frac{2\xi_n h}{d}\right)\right]^2 \tag{3}$$

In the above equations, m_{liq} is mass of the liquid, ξ_n are the roots of specific Bessel functions, g is gravity's acceleration and *tanh* is the hyperbolic tangent function.

Structural dynamic model

Dynamic Equation of Motion

According to Craig and Kurdila, (2006), the motion of complete system is represented by:

$$[M]\{\ddot{u}(t)\} + [C]\{\dot{u}(t)\} + [K]\{u(t)\} = \{F(t)\} \tag{4}$$

where, $[M]$, $[C]$ and $[K]$ are, respectively, mass, damping and stiffness matrices. Displacements, velocities, and accelerations are represented by $\{u(t)\}$, $\{\dot{u}(t)\}$ and $\{\ddot{u}(t)\}$, respectively. On the right hand side $\{F(t)\}$ represents the forces acting on the system.

Transient Response Analysis

Considering a time domain analysis (transient response), to evaluate the shifted response of Eq. (4) numerical integration is performed. Two methods can be used: Direct Transient Response and Modal Transient Response. As the finite element model of the launch vehicle has a small number of degrees of freedom, and in order to obtain greater accuracy, we performed a Transient Modal Response Analysis using the Central Difference Method.

The Central Difference Method

According to Komzsik, (2013), the method is based on the 3-point central difference formula for the first and second order numerical derivatives as:

$$\{\dot{u}(t)\} = \frac{1}{2\Delta t}\{u(t+\Delta t) - u(t-\Delta t)\} \tag{5}$$

and

$$\{\ddot{u}(t)\} = \frac{1}{\Delta t^2}\{u(t+\Delta t) - 2u(t) + u(t-\Delta t)\} \tag{6}$$

In the central difference method the equilibrium of the system is considered at time t and the displacements are calculated at time $t+\Delta t$, where the Δt is the equidistant time step, hence this is an explicit time integration scheme. Substituting into the equilibrium equation at t we get:

$$[M]\frac{1}{\Delta t^2}\{u(t+\Delta t) - 2u(t) + u(t-\Delta t)\} + [B]\frac{1}{2\Delta t}\{u(t+\Delta t) - u(t-\Delta t)\} + [K]\{u(t)\} = F(t) \tag{7}$$

Reordering yields:

$$\left[\frac{1}{\Delta t^2}[M] + \frac{1}{2\Delta t}[B]\right]\{u(t+\Delta t)\} = \{F(t)\} + \left[\frac{2}{\Delta t^2}[M] - [K]\right]\{u(t)\} - \left[\frac{1}{\Delta t^2}[M] + \frac{1}{2\Delta t}[B]\right]\{u(t-\Delta t)\} \tag{8}$$

Transient loads

During ascent flight, a launcher vehicle experiences different dynamics loads NASA-HDBK, (2001). In this sense, the turbulent atmosphere is the major source due to wind gust presence.

According to Kabe and Sako, (2020), a launcher vehicle, takes very little time within any altitude band and, therefore, turbulence must be treated as short duration, nonergodic transient. In addition, a launch vehicle's flight control system is an integral part of its low-frequency dynamic response. Hence, launch vehicle turbulence/gust must be computed numerically in the time domain.

Synthetic gust profiles

If measured winds data are not available, synthetic profiles that are intended to yield conservative responses could be used. Two such profiles used for launch vehicle loads analysis are *one-minus cosine* an the *one-minus cosine flat-top*, Fig.4 , Kabe and Sako, (2020).

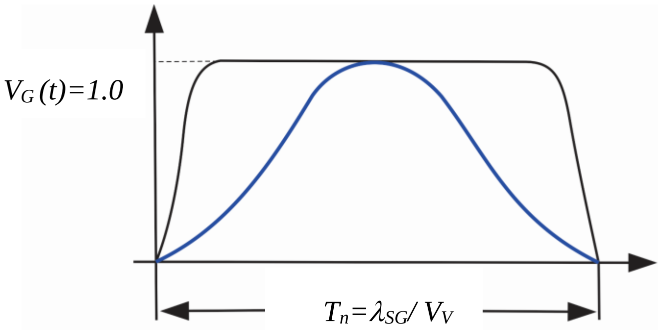

Figure 4 – Synthetic gust profile, "Kabe and Sako, (2020)

The one-minus cosine profile is defined as:

$$\{V_G(t)\} = \begin{Bmatrix} \frac{1}{2}A_G\left(1 - cos\frac{2\pi}{T_n}t\right) & 0 \le t \le T_n \\ 0 & otherwise \end{Bmatrix} \tag{9}$$

The amplitude A_G requires that we compute the profile wave length, λ_{SG}, i.e., λ_{SG}, $=T_nV_v$, where V_v is the speed of the vehicle and T_n is the period of vibration of the mode to which the profile is "tuned".

The *one-minus cosine* with flat-top is defined as:

$$\{V_G(t)\}=\begin{Bmatrix} \frac{1}{2}A_G\left(1-cos\frac{2\pi}{T_n}t\right) & 0\le t\le 0.1T_n \\ A_G & 0.1T_n\le t\le 0.9T_n \\ \frac{1}{2}A_G\left(1-cos\frac{2\pi}{T_n}t\right) & 0.9T_n\le t\le T_n \\ 0 & otherwise \end{Bmatrix} \tag{10}$$

Aerodynamic load

The effect of wind gust should be factored in the load analysis, as pointed out in Chin, S.S., (1961). This may be done by increasing the angle of attack by an incremental value defined below:

$$\alpha_G = \frac{V_G}{V_V} \tag{11}$$

where α_G is the angle of attack due to gust and V_v is the velocity of the launcher vehicle. The lateral aerodynamic force in a determined station along the launch body is given by:

$$F_j(t)=q\,S_{ref}\left(C_{N\alpha j}\right)\alpha_G \tag{12}$$

where q is the dynamic pressure, S_{ref} the reference area and $CN_{\alpha j}$ is aerodynamic coefficient for a station j. Combining Eqs.(10),(11) and (12) the transient aerodynamic force due to wind gust given by:

$$F_j(t)=q\,S_{ref}\left(C_{N\alpha j}\right)\left(\frac{V_G(t)}{V}\right) \tag{13}$$

In this work, we calculated local normal force coefficient CN_j for a station j, which take into account a specific angle of attack, at an predefined altitude and Mach. This task was performed through a routine developed in the numerical computation software MATLAB, (2014). In this case, the peripheral pressure coefficient distributed on determined station along the body produced by Missile Datcon, Blake, W.B., (1997), The local normal-force coefficient per length unit may determined as follow, Chin, S.S., (1961):

$$C_N = \frac{2r}{S}\int_0^{\pi} c_p\, cos\theta\, d\theta \tag{14}$$

where r is the radius of the body, S is the area and c_p is coefficient of pressure given by:

$$c_p = \frac{(p-p_0)}{q_0} \tag{15}$$

where p is the pressure on body surface station, p_0 reference pressure and q_0 is dynamic pressure reference. The value of CN_j is next plotted v. body station as shown in Fig.5.

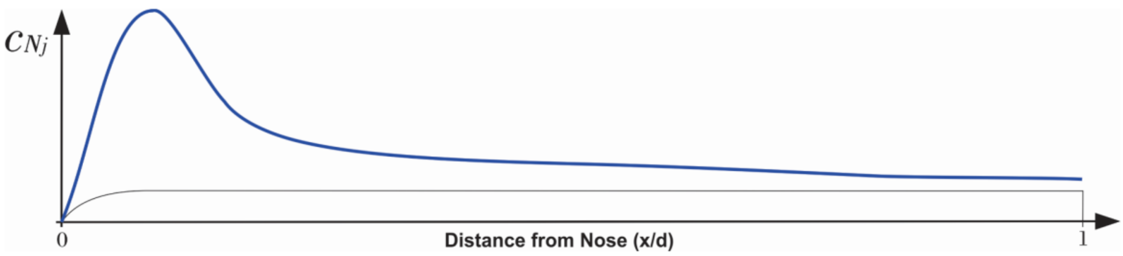

Figure 5 – Variation of local normal-force coefficient with body station

Flight conditions

The available trajectory data of a conceptual launcher vehicle present in Zhuang and Yulin, (2021) were used. The maximum dynamic pressure is considered as flight critical condition. Thus, the variation of local normal-force coefficient were determined considering the altitude, Mach number and a fixed angle of attack. For a sensitivity analysis of slosh effects, the same aerodynamic loads are applied on body vehicle for different fill ratios of the propellant tanks during first stage flight.

Table 1 contain the parameter used to calculate local normal-force aerodynamic coefficients for critical flight conditions.

Table 1 – Trajectory parameters, Zhuang and Yulin, (2021)

Time(s)	Altitude (m)	Mach	q_{max} (Pa)	α (º)
75.0	110000.0	1.4	44500.0	3.0

Finite element model

The data used for constructed the launcher vehicle model in commercial package Nx Nastran, (2014); they are these available in Zhuang and Yulin, (2021). Due to large (L/D) ratio the beam model is adequate for capturing the flexibility effects. The propellant can be considered as rigid or distributed mass on the idealized beam while a smaller portion must be allowed to sloshing in the lateral model. Basically, beam elements, lumped mass element and linear spring elements were used, Fig. 6. The launcher vehicle model contain a total of 172 elements.

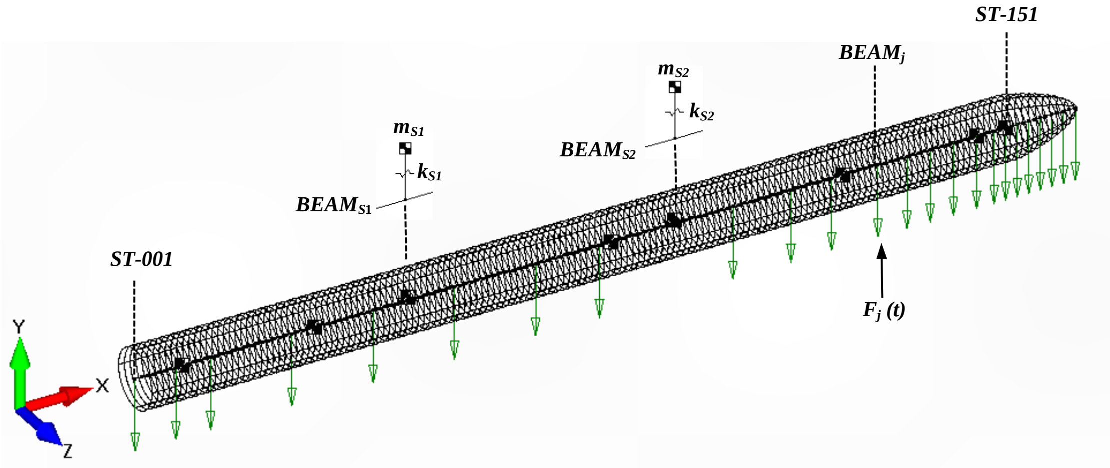

Figure 6 – Finite element model

Modal analysis

In Aguiar and Souto, (2021), the mode shape and natural frequencies of the same launcher vehicle, Fig.6, were calculated. Behavior vibration of slosh and structural bending were founded. These dynamic characteristics change with time and they were stablished for respective fill ratios of 75%, 50% and 25%.

The Table 2 presents the natural frequencies for both dynamic characteristics. These frequencies should be tuned to calculate the wind gust profile, Fig 4, for transient analysis.

Table 2 – Natural frequencies, Aguiar and Souto, (2021)

Dynamic Characteristic	Sloshing		Bending	
	Mode 1	Mode 2	Mode 1	Mode 2
FR (%)	f_{b1}(Hz)	f_{b2}(Hz)	f_{S1}(Hz)	f_{S2}(Hz)
75.0	1.318	1.338	8.416	33.146
50.0	1.140	1.166	8.862	34.338
25.0	1.021	1.093	11.752	34.912

RESULTS

The simulation results were calculated with the transient response solution (SOL109) of the Nx Nastran, (2014).The accelerations were obtained with respect to two distinct points of the finite element model, Fig.6. The first point is the engine support structure (ST-001) and the second one is the payload support structure (ST1-151). These points are important for the launcher vehicle's development, mainly during its preliminary phase. In fact, they are related to design requirements for the control system frequency and for the dynamic environment at the payload, respectively. The Fast Fourier Transform (FFT) of acceleration at both points was calculated in order to identify the response frequencies.

Simulation (I): Transient response: sloshing frequencies

The launcher vehicle was submitted to the following wind gust profiles: (a) one-minus cosine and (b) flat-top, Fig.4. The first sloshing frequency was taken into account as tuning frequency with respect to the fill ratio, Tab.2. Figure 11 presents results related to the engine support structure (ST-001) and Fig. 12 presents results for the payload support structure (ST-151).

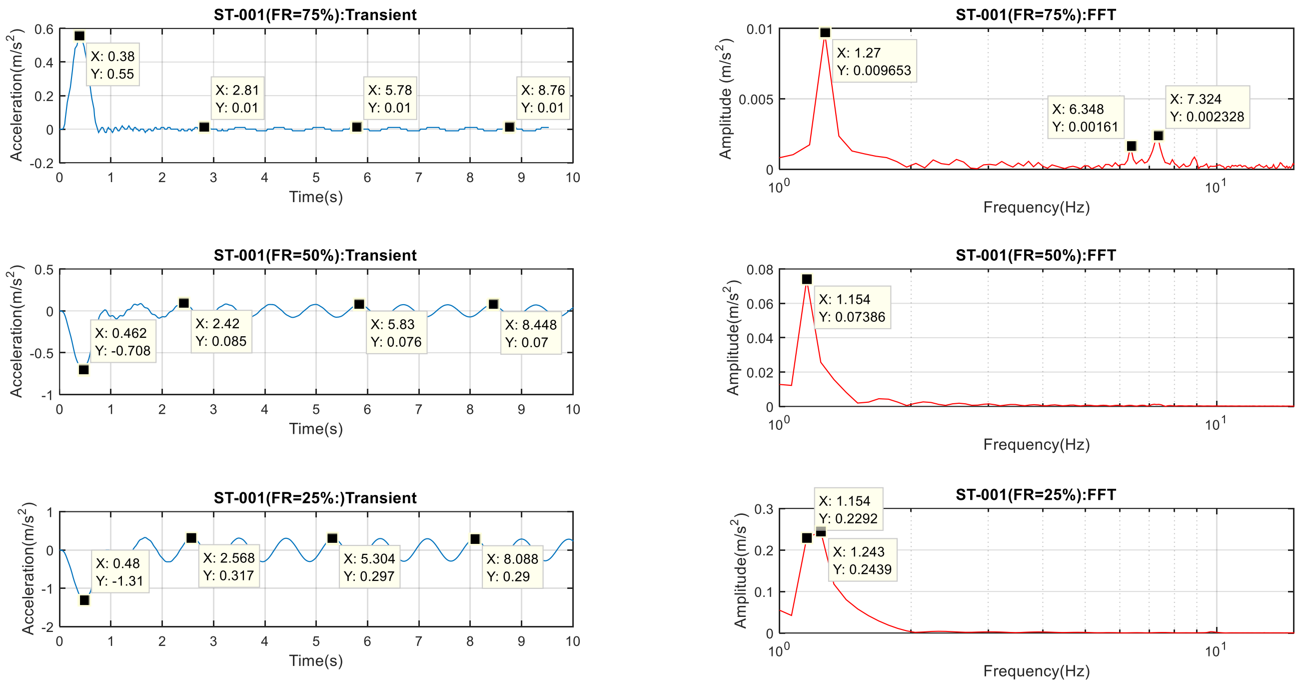

(a)

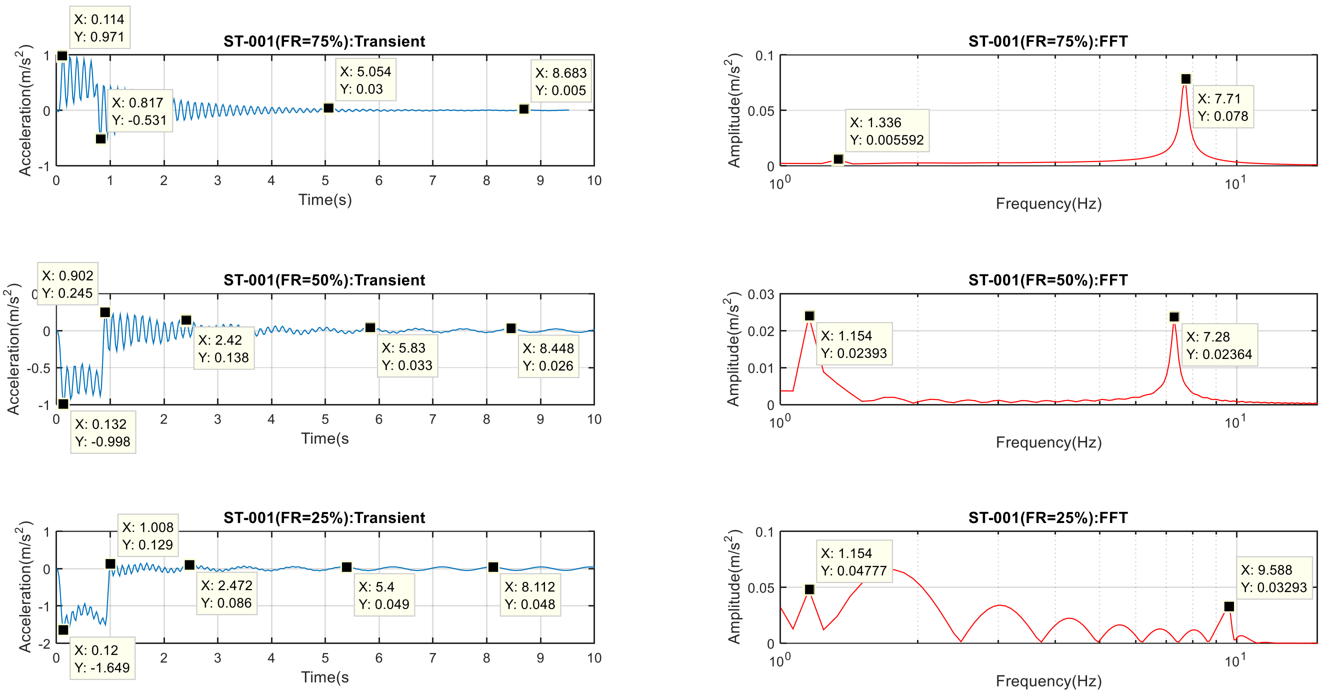

(b)

Figure 11 – Time responses (in blue) and its FFT (in red) in the point ST-001 (f_{S1})

(a) one-minus cosine (b) flat-top

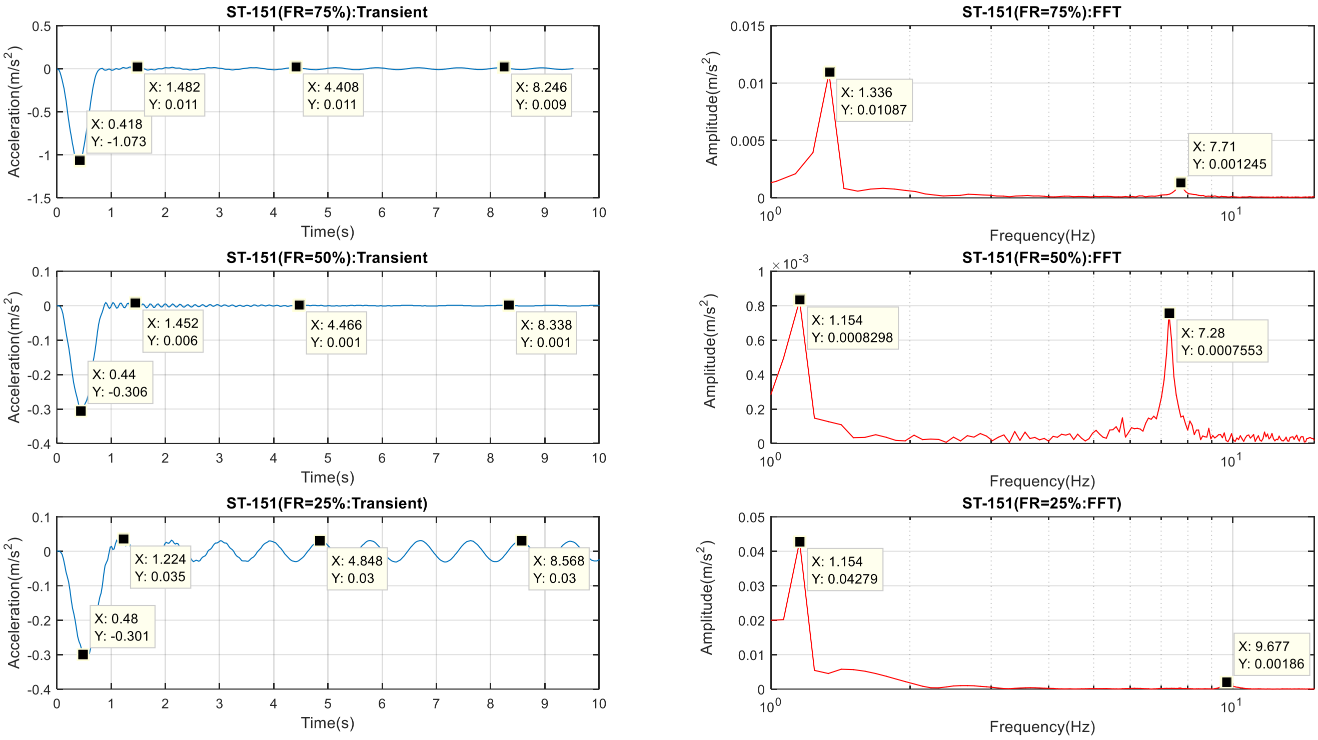

(a)

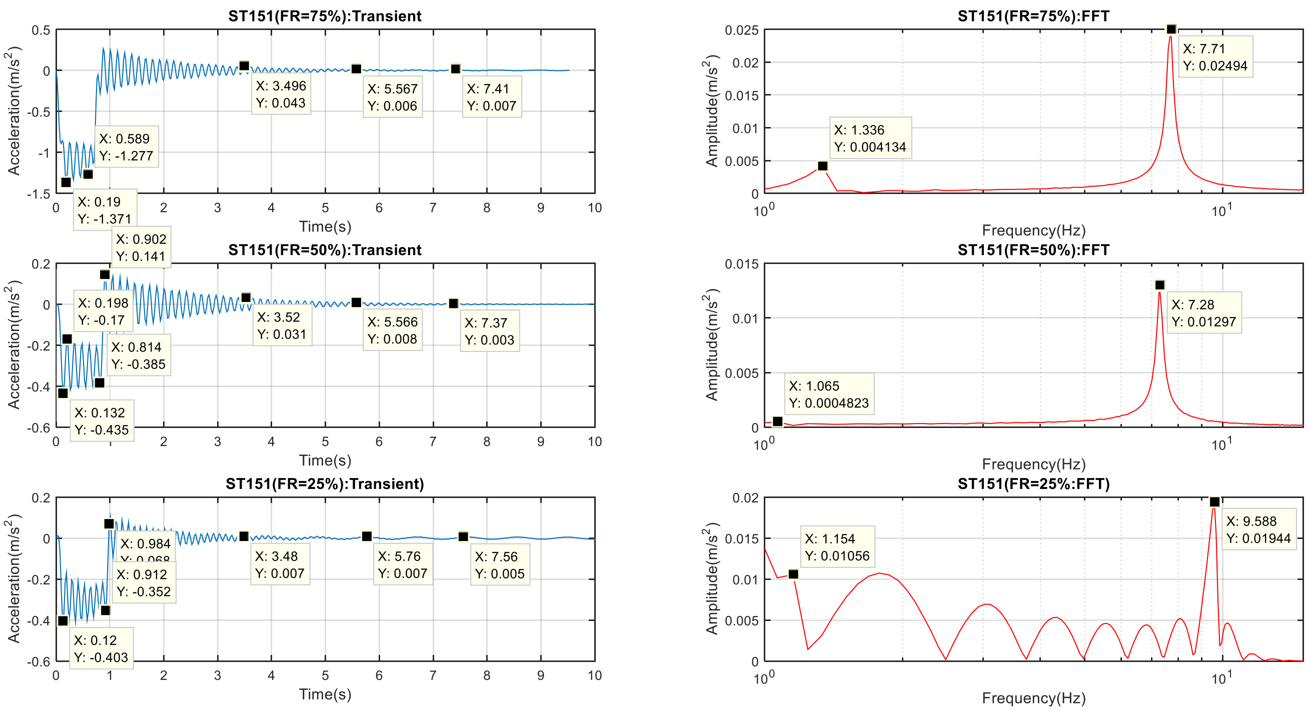

(b)

Figure 12 – Time responses (in blue) and its FFT (in red) in the point ST-151 (f_{S1})

(a) one-minus cosine profile (b) flat-top

Simulation (II): Transient response: structural bending frequencies

Only the payload (ST-151) was considered due to their bending's frequencies are more close these related to its dynamic environment. This analysis compares the acceleration response for two different conditions: when the slosh mass is fixed to the vehicle´s body and when it is free to oscillate. For this case, the excitation is a one-minus cosine gust profile with frequency of the first bending frequency, Tab.2. The Figures 13–15 present the results for the fill ratios.

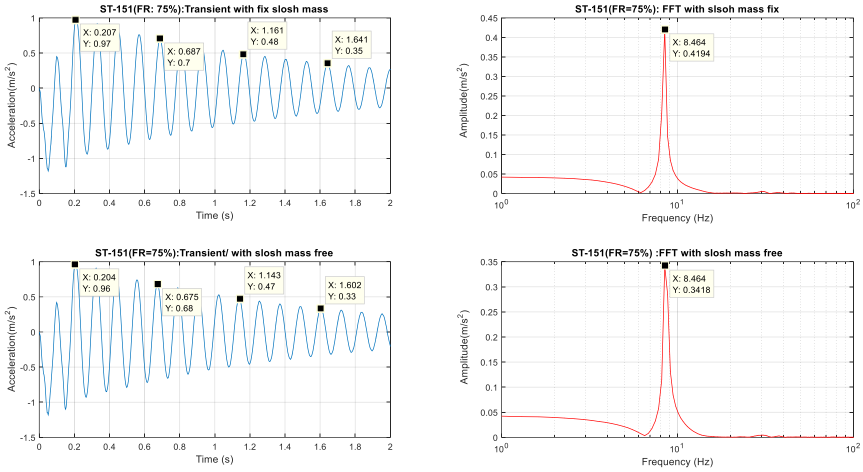

Figure 13 – Time responses (in blue) and its FFT (in red) in the point ST-151 (f_{b1}): FR = 75%

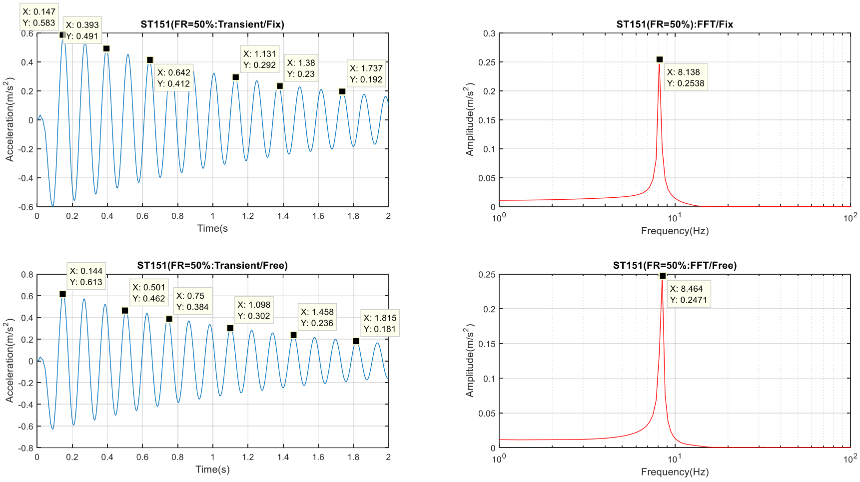

Figure 14 – Time responses (in blue) and its FFT (in red) in the point ST-151 (f_{b1}): FR = 50%

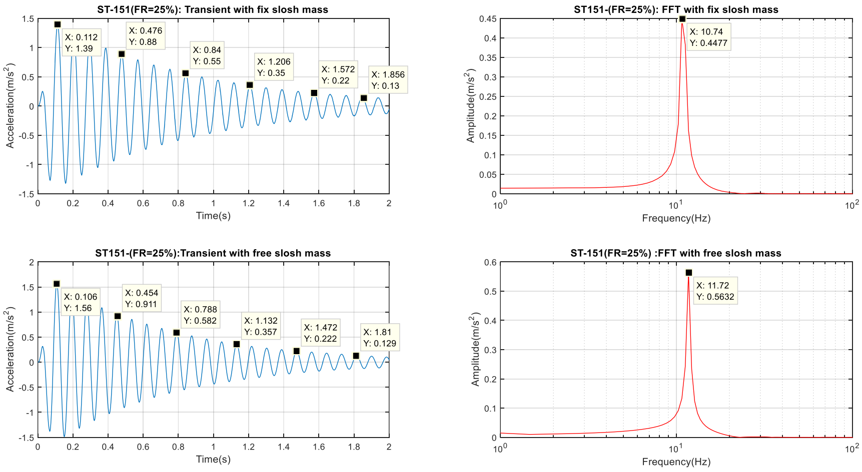

Figure 15 – Time responses (in blue) and its FFT (in red) in the point ST-151 (f_{b1}): FR = 25%

Remarks

Simulation (I): In general, considering the time domain analysis: (a) flat-top gust profiles produce accelerations higher than one-minus minus cosine gusts, (b) As it would be expected, acceleration responses decreased with time due to an imposed stiffness-proportional damping of 2% at the first sloshing frequency. The acceleration responses at ST-001 increased as the fill rate decreased. However, at ST-151 variations occurred, with FR= 50% presenting slightly higher accelerations than FR=25%. In frequency-domain analysis, response peaks with values close to the first launcher vehicle's sloshing mode were identified for all fill ratios. In some cases, peaks with frequencies close to the vehicle's first bending mode were also observed, mainly in the responses calculated for the station ST-151.

Simulation (II): In time-domain analysis, the acceleration decreased due to structural damping, as above-mentioned. The oscillation condition with free slosh masses provided greater acceleration responses than when masses are fixed to the launcher's body, especially when filling rates were increased. From the frequency-domain analyses, it was identified that, for all fill ratios, the free slosh masses oscillate in frequencies close to the first structural bending mode.

CONCLUSIONS

The methodology described can be applied during preliminary design's phase to analyze the dynamic behavior of a launch vehicle with lateral sloshing effects during the ascending flight through the atmosphere. Thus, the acceleration responses in critical regions along the vehicle's body are analyzed. For example, the engine point and payload point were chosen due to their design requirements. The vehicle was submitted to transient load originating from two types of discrete wind gust (a one-minus cosine and a flat top) as a forcing function. Configurations with 3 tank filling ratios (25%, 50% and 75%) were studied in order to verify the sloshing effects. Overall, for most fill ratios, the one-minus cosine burst excited the sloshing modes more intensely than the flat top burst. This last one excited mainly the vehicle's bending modes. For the 50% fill ratio, the sloshing and bending modes responded with similar magnitudes. In future works, it is also intended to include the effects of forces originated from the vehicle's control system.

ACKNOWLEDGMENTS

This study was financed in part by the Coordenação de Aperfeiçoamento de Pessoal de Nível Superior - Brasil (CAPES) - Finance Code 001.

REFERENCES

Abramson, H.N., 1966, "The dynamic behavior of liquids in moving containers: with applications to space vehicle technology", NASA SP-106.

Aguiar, D.S. and Souto, d'A C, 2021, "Dynamic of Launch Vehicle with Slosh Effects". CILAMCE-PANACM, Rio de Janiro.

Barrows, T. and Orr, J. 2021, "Dynamic and Simulation of Flexible Rockets", Elsevier Inc.

Blake, W.B., 1997, Missile Datcom – User's Manual. Ohio. Rright-Patterson AFB, (AFRL-VA-WP-TR-1998-3009)

Chin, S.S., 1961,"Missile Configuration Design. McGraw-Hill Book Company, New York

Craig Jr, R.R. and Kurdila, A.J., 2006, "Fundamentals of Structural Dynamics". John Wiley and Sons- Second Edition.

Dodge, F., 2000. "The New Dynamic Behavior of Liquids in Moving Containers," Southwest Research Institute.

FEMAP Nx Nastran, 2014, "Educational License".

Ibrahim, R.A, 2005, "Liquid Sloshing Dynamics – Theory and Applications" – Cambridge.

Jayasidhan, A. K, Jancy Rose, K, R, Neetha, R., 2015, "Dynamic Response of a Launch Vehicle to Wind Gust", International Journal of Engineering Development and Research – IJEDR, Volume 3, Issue 3.

NASA-HDBK -7005, 2001," Dynamic Environmental Criteria" NASA Technical Handbook.

Schlingloff, H., 2005,"Astronautical Engineering – An introduction to the Technology of Spaceflight" Bad Abbach, Germany.

Shimote, W. K. 2005 "Rocket Propulsion Course Notes", Institute of Aeronautics and Space, São José dos Campos, SP, Brazil

Steny, Babu G., Rajendaru P., Nair, R.P., 2020, "Dynamic Load Factor of a Typical Launch Vehicle during Atmospheric Phase" – International Research Journal of Engineering and Technology (IRJET), Volume: 07 Issue: 05, May.

Suresh, B.N.; Sivan, K., 2015, "Integrated Design for Space Transportation System", Springer India 2015

Zhuang, L. and Yulin, Z., 2021, "Deformation Reconstruction and High-Precision Attitude Control of a Launch Vehicle Based on Strain Measurements." International Journal of Aerospace Engineering – Hindawi. February.

RESPONSIBILITY NOTICE

The authors are the only parties responsible for the printed material included in this paper.